JPET Fast Forward. Published on October 1, 2007 as DOI: 10.1124/jpet.107.128587

JPET#128587

Antimetastatic effect of a small molecule vacuolar H^+-ATPase inhibitor in *in vitro and in vivo* preclinical studies

Rosanna Supino, Giovanna Petrangolini, Graziella Pratesi, Monica Tortoreto, Enrica Favini, Laura Dal Bo, Patrizia Casalini, Enrico Radaelli, Anna Cleta Croce, Giovanni Bottiroli, Paola Misiano, Carlo Farina, Franco Zunino

Fondazione IRCCS Istituto Nazionale Tumori, Milan, Italy (R.S., G.Pe., G.Pr., M.T., E.F., L.D.B., P.C., F.Z.); Facoltà Medicina Veterinaria Università degli Studi di Milano, Milan, Italy (E.R.); Consiglio Nazionale delle Ricerche, Università di Pavia, Pavia, Italy (A.C.C., G.B.); Nikem Research, Baranzate, Milan, Italy (P.M., C.F.)

JPET Fast Forward. Published on October 1, 2007 as DOI: 10.1124/jpet.107.128587
This article has not been copyedited and formatted. The final version may differ from this version.

Running title: Antimetastatic effects of vacuolar H+-ATPase inhibition

Abbreviations: dimethyl sulfoxide, DMSO; microvessel density, MVD; phosphate buffered solution, PBS.

Corresponding author: Franco Zunino, Fondazione IRCCS Istituto Nazionale Tumori, Via Venezian 1, 20133 Milan, Italy. Tel. +39-02-23902267; Fax +39-02-23902692; e.mail franco.zunino@istitutotumori.mi.it

Text pages: 29

Tables: 1

Figures: 9

References: 33

No. of words in the Abstract: 174

No. of words in the Introduction: 429

No. of words in the Discussion: 1104

Section assignment: Chemotherapy, Antibiotics and Gene Therapy

Abstract

On the basis of the evidence that vacuolar H^+-ATPase is implicated in the development of the metastatic phenotype, we have explored the possibility to target the enzyme function in an attempt to control the metastatic behaviour of tumor cells. In this study we used an indole derivative, NiK-12192 [4-(5,6-dichloro-1*H*-indol-2-yl)-3-ethoxy-*N*-(2,2,6,6-tetramethyl-piperidin-4-yl)-benzamide], recently identified as an effective inhibitor of vacuolar H^+-ATPase, as a potential antimetastic agent in the treatment of NSCLC H460 xenograft, which is able to induce lung metastases in mice. Oral administration of NiK-12192 caused a significant inhibition of formation of spontaneous metastases. In contrast, the drug exhibited a negligible effect on the development of artificial metastases (i.e. following i.v. injection of tumor cells), thus supporting that the drug affect the early events of the metastatic process (e.g., migration and invasion). Cellular effects are consistent with this interpretation. In conclusion, the available results show for the first time that a vacuolar H^+-ATPase inhibitor is effective in modulation of the metastatic behaviour of a lung carcinoma, supporting its potential therapeutic interest as a novel treatment approach.

JPET Fast Forward. Published on October 1, 2007 as DOI: 10.1124/jpet.107.128587
This article has not been copyedited and formatted. The final version may differ from this version.

Introduction

The metastatic process occurs through a cascade of events involving a complex series of interactions with the host tissues allowing migration and invasion of tumor cells (Liotta and Stetler-Stevenson, 1993). The acidic extracellular microenvironment, which characterizes the solid tumors, is recognized to be a critical factor in stimulating tumor cell motility and invasive behaviour (Harguindey et al., 2005). Indeed, the acidification of the hypoxic extracellular microenvironment facilitates the action of the acidic proteases, as well as cell locomotion (Rozhin et al., 1994; Martinez-Zaguilan et al., 1996; Stock et al., 2005; Rofstad et al., 2006). Acidification of extracellular microenvironment reflects homeostatic mechanisms regulated by proton exchangers or proton pumps.

Proton transporters implicated in pH regulatory mechanism include the Na^+/H^+-exchanger, Na^+/K^+-ATPase pump, vacuolar H^+-ATPases, H^+/Cl^- symporter and proton lactate symporters (Putnam, 2001; Harguindey et al., 2005). The vacuolar H^+-ATPase, is expressed in plasma membrane and cytoplasmic organelles and can contribute to the metastatic potential of many tumor cells (Sennoune et al., 2004a; Sennoune et al., 2004b; Martinez-Zaguilan et al., 1993; Martinez-Zaguilan et al., 1998). On the basis of its function, it is conceivable that inhibition of vacuolar H^+-ATPase function/expression may affect the invasive behavior of tumor cells. Indeed, the knocking down of ATP6L, the 16 kDa subunit of vacuolar H^+-ATPase, in a human hepatocellular carcinoma cell line resulted in inhibition of growth and metastases in nude mice (Lu et al., 2005). In clinical specimens, vacuolar H^+-ATPase was detected in invasive pancreatic carcinomas (Ohta et al., 1996).

We have recently reported that the vacuolar H^+-ATPase inhibitor NiK-12192, a lead compound of a novel series of substituted indole derivatives (Farina et al., 2001), was able to

potentiate the antitumor activity of the camptothecin topotecan at well-tolerated doses (Petrangolini et al., 2006). Although NiK-12192 exhibits a marginal effect on the s.c.-growing tumor xenografts, the intra/extra-cellular modulation of pH is expected to influence spreading of tumor cells and metastasis development. The present study was based on the hypothesis that inhibition of vacuolar H^+-ATPase, which has a prominent role in modulating the pH gradient, may influence the metastatic behaviour of tumor cells. Therefore, aim of the study was to investigate the role of NiK-12192 on the growth and the metastatic spreading of a human lung tumor, H460, which is able to form spontaneous lung metastases when implanted s.c. in nude mice (Corti et al., 1996). The results indicated that oral treatment with NiK-12192 resulted in a relevant antimetastatic effect in animal models. Moreover, in vitro studies confirmed the inhibitory activity of the compound in various assays designed to investigate cellular effects relevant to the metastatic behaviour.

Material and Methods

Drugs. NiK-12192 and topotecan used in this study are products of Nikem Research, Milan and Glaxo SmithKline, Verona, Italy, respectively. Bafilomycin A1 is provided by Sigma-Aldrich (St. Louis, MO).

For *in vitro* studies, stock solutions (1 mg/ml) were stored in DMSO for NiK-12192 and diluted before use in saline solution. In experiments, the final concentration of DMSO in the medium was 0.1%, which has been verified to be non toxic in our cell system.

For *in vivo* studies, NiK-12192 was dissolved by adding absolute ethanol and Cremophor ELP (both 5% of the final volume) and diluted (just before use) by adding 0.9% NaCl. Topotecan

JPET Fast Forward. Published on October 1, 2007 as DOI: 10.1124/jpet.107.128587
This article has not been copyedited and formatted. The final version may differ from this version.

was dissolved in sterile distilled water.

H460 human tumor model system. The NCI-H460 non small cell lung tumor cell line (hereafter named H460) was used in the *in vitro* studies. For animal experiments, H460 tumor cells were adapted to grow as ascitis in nude mice, and maintained *in vivo* by i.p. passages ($5x10^6$ cells/mouse in 0.5 ml PBS). Briefly, cells were collected from the donor mice about 7 days after inoculum and, after washing, cell number and viability were determined by trypan blue exclusion. Cell suspension was injected s.c or i.v. in order to achieve spontaneous or experimental metastases (Cassinelli et al., 2006).

In vitro studies

Intracellular pH determination. Cells grown on coverslips were incubated for 40 min with SNARF-4F (5-(and -6) carboxilic acid, acetoxymethyl ester, acetate, stock solution (80 mM in DMSO); Invitrogen, Eugene, OR) at the final concentration of 8 μM. Dilutions were performed directly in the medium deprived of serum, to prevent the hydrolysis of the fluorogenic substrate. After incubation, the coverslips were rinsed with PBS and mounted upside down on the microscope slides. SNARF-4F incubation was performed on control (untreated) cells and on cells pretreated with NiK-12192 (2 μM, 24 h) (Marcotte and Brouwer, 2005). Microspectrofluorometric analysis was performed under epi-illumination conditions by means of a Leitz microspectrograph (Wetzlar, Germany) equipped with an Optical Multichannel Analyzer (OMA, EG&G, mod. 1420/512; Princeton Applied Research, Princeton, NJ). Excitation light was provided by a 100 W Hg lamp (Osram, Berlin, Germany), combined with KG1 and BG38 anti-thermal filters, and selected by a 366 nm interference filter (T% = 25). Fluorescence spectra were

recorded from single cells (cytoplasmic area selected by means of a field diaphragm) in the 550-800 nm interval. The intracellular pH values were estimated from the blue shift of the emission band centered at about 655 nm at pH 7.2, according to the reference spectra reported by the dye producer. Measurements were performed by means of an oil-immersion Fluotar Leitz objective (100X NPL, incorporated iris diaphragm; NA 0.60-1.32).

Vacuolar H^+-ATPase expression and subcellular localization. For vacuolar H^+-ATPase expression, western blot analysis was performed after 24h of treatment with Nik-12192 (2 μM), as already reported (Zuco et al., 2004). Anti-vacuolar H^+-ATPase D primary antibody (Sc-20945; Santa Cruz Biotechnology, Santa Cruz, CA) was used.

For subcellular localization of the protein, cells were seeded on coverslips in 6 multi-well plates, treated for 24 h, fixed in paraformaldehyde 4%, and then incubated for 60 min with vacuolar H^+-ATPase antibody. After washing in PBS containing 1% bovine serum albumine, samples were incubated with the FITC-secondary anti-rabbit antibody (Invitrogen) and mounted with Mowiol (Mowiol 4.88, Calbiochem) and observed by fluorescence microscope DMRB (Leitz). Images were taken by a 50x immersion oil objective, with an excitation light provided by a 100 W Hg lamp and an excitation filter at 450-490. Images were recorded with a Spot Insight digital camera (Delta Sistemi, Roma, Italy) equipped with a system of image analysis (IAS 2000, Delta Sistemi).

Migration and invasion assays. H460 tumor cells were seeded in complete medium and, after 24h, treated with different concentrations of the drug for 24 h. Then, cells were harvested and transferred in the upper chamber of 24 well Transwell plates (Costar, Corning Incorporated, Corning, NY) in serum-free medium ($1.2x10^5$ cells/well), whereas conditioned medium was

added to the lower chamber. To maintain cells under drug exposure during the assay, the drug was added in the upper and lower compartment of the chambers at the same concentration as in the previous treatment. In migration assay, after 5 h of incubation at 37^{o}C, filters were cleaned on the upper side with a cotton swab, fixed in 99% ethanol, stained with a solution of sulphorodamine B 0.4% in acetic acid 1% and migrated cells were counted under an inverted microscope. All experiments were performed 3 times in duplicate.

In the invasion assay, the procedure was the same as described above, except that the Transwell chamber membranes were coated with 12.5 µg of Matrigel/well (BD Biosciences, San Jose, CA) and that the Transwell plates were processed after 24 h of incubation at 37^{o} C.

Wound healing assay. H460 tumor cells were seeded onto 24-well plates at 4.5x10^{5} cells/well in growth medium. A single scratch wound was created on confluent monolayers by using a micropipette tip (Liang et al., 2007). Cells were washed with PBS to remove cell debris, supplemented with serum-free medium containing NiK-12192, and monitored. Images were captured by a Spot Insight digital camera (Delta Sistemi) using a 4x contrast phase objective at 0 and 48 h post wounding and wound distance (µm) was measured by system of image analysis (IAS 2000). Three different regions for each wound were considered. The experiment was performed two times.

αvβ3 expression and cellular localization. Cells, seeded on coverslips in 6 multi-well plates were treated with NiK-12192 (2 µM). After 24h of drug exposure, samples were incubated with a solution 1:400 of FITC-conjugated mouse anti-human-αvβ3 monoclonal antibody (Mab1976F, Chemicon International, Temecula, CA) for 1h, mounted with Mowiol and observed

by fluorescence microscope as above reported.

Tubulin and actin microscopic analysis. For confocal experiments, cells were grown on coverslips, treated with NiK-12192 (2 μM) for 24 h, fixed with 4% paraformaldehyde for 30 min, and then washed and added with 70% ethanol for 20 min at -20°C. After washing with PBS containing 1% bovine serum albumine, cells were incubated with phalloidin, fluorescein-isothiocyanate-labeled 1:200 (Sigma-Aldrich) and monoclonal anti-β-tubulin 1:2000 (clone SDL3D10, Sigma) for 1h at 37°C. Samples were then incubated with Alexa 594-conjugated anti-mouse IgG antibody (Invitrogen) for 30 min, mounted with Prolong Gold Antifade reagent (Invitrogen) and analyzed by confocal microscopy (Microradiance 2000; Bio-Rad Laboratories, Inc., Hercules, CA) equipped with Ar (488 nm) and HeNe (543 nm) lasers. Images (1024 x 1024 pixels) were obtained using a 60x oil immersion lens and analyzed using Lasersharp 2000 software. Reported images represent a single Z-section of the samples with 0.5 μm step. The pinhole diameter was regulated according to the value suggested by the acquisition software to obtain the maximum resolution power.

Three-dimensional cell culture. H460 tumor cells ($0.8x10^4$ cells/plate) were cultured in bacteriological plates (5 cm diameter) in complete culture medium. After 6 days, single spheroids were transferred to 96-well plates in culture medium containing NiK-12192 at different concentrations. Measures of spheroid diameters were taken by a micrometer lens in the inverted microscope at 0, 24, 48 and 72 h. Values are reported as mean percentage of the diameter length over that of time 0 (100%). Six spheroids for each point were considered.

JPET Fast Forward. Published on October 1, 2007 as DOI: 10.1124/jpet.107.128587
This article has not been copyedited and formatted. The final version may differ from this version.

In vivo studies

Animals. All experiments were carried out using female athymic nude CD-1 mice, 8-11 weeks old (Charles River, Calco, Italy). Mice were maintained in laminar flow rooms with constant temperature and humidity. Experimental protocols were approved by the Ethic Committee for Animal Experimentation of the Istituto Nazionale Tumori (Milan, Italy), according to the United Kingdom Coordinating Committee on Cancer Research Guidelines (Workman et al., 1998).

Antitumor and antimetastatic activities. The effects of NiK-12192, topotecan, or combination of them on the growth of primary tumors and spontaneous lung metastases were tested in mice inoculated s.c. in the right flank with H460 ascitic tumor cells ($2x10^6$/mouse). Each control or drug-treated group included 9-11 mice. The growth of the s.c. tumor was followed by biweekly measurements of tumor diameters with a Vernier caliper. Tumor weight (TW) and TW inhibition percentage (TWI%) in treated over control mice were calculated as previously reported (Cassinelli et al., 2006). Drug treatment was delivered per os, by gavage, daily for 9 weeks (week-ends excluded), starting the day after cell injection (day 1). NiK-12192 was delivered at the dose of 30 mg/kg, topotecan at the dose of 1 mg/kg. In the mice treated with the combination NiK-12192 was delivered about 1 h after topotecan. At day 63, tumor-bearing mice were sacrificed by cervical dislocation and their lungs removed. Lung lobes were spliced between two glass slides and the metastatic nodules were macroscopically counted against a bright light. Reading of metastases was performed by two independent observers, unaware of the experimental group, with an interobserver reproducibility >95%. The metastatic nature of these areas was confirmed by histological analysis.

To induce experimental lung metastases, mice (7-8/group) were injected i.v. with ascitic

H460 cells ($2x10^6$/mouse) (Cassinelli et al., 2006), and then treated per os, daily, with NiK-12192 (30 mg/kg), and/or topotecan (1 mg/kg) for 7 weeks (week-ends excluded), from day 1. At day 83 all mice were sacrificed for lung observation as described above. In the presence of confluent metastatic nodules, lungs were defined as "tumor invaded" and tumor nodules not counted. The number of 500 metastases was ascribed. For ethical reasons, mice presenting signs of suffering were sacrificed before day 83.

For histological observation, s.c.-implanted tumor-bearing mice (3-4 mice/group) were treated with NiK-12192 (30 mg/kg) alone or in combination with topotecan (1 mg/kg), daily for 2 weeks, starting at day 1. The day after the last treatment, mice were sacrificed and their tumors excised and fixed in 10% buffered formalin for hematoxylin-eosin staining. Angiogenesis was analyzed by detection of microvessel density (MVD). Number of blood vessels was assessed in three fields, at 400x, within non necrotic areas. Only vascular units containing erythrocytes were considered (Belotti et al., 1996).

Statistical analysis. The Student's t test was used to compare TW in control and treated mice. The number of metastases and microvessels in control and treated mice was compared by the Mann-Whitney test. All analyses were performed using Graph Pad Prism software (Graph Pad Prism Inc. S.Diego, CA).

Results

Modulation of intracellular pH. NiK-12192 was able to decrease the intracellular pH, as assessed by means of the pH-dependent shift of the SNARF-4F emission band through the

microspectrofluorometric analysis. Indeed, as shown in Fig. 1, in NiK-12192 treated cells the pH-probe exhibited a shift to shorter wavelengths consistent with a more acidic pH environment with respect to the control cells. The emission peak position of control cells was constant at about 650 nm, whereas those of the cells treated for 24h with NiK-12192 (2 μM) were always comprised between 640 and 630 nm. The estimation of the intracellular pH value was performed exclusively on the base of the blue shift of the SNARF-4F longer emission band, and indicated a decrease from about 7.2 for the control to a pH range of about 6.2 for NiK-12192 treated cells. The increase in the emission band centered at about 560 nm was not considered, since it can be due both to the conversion of SNARF-4F emission at acidic pH and to a shoulder of the NiK-12192 emission. Although the level of vacuolar H^+-ATPase expression was not modified by treatment with the compound (Fig. 2A), NiK-12192 produced changes in intracellular localization (Fig. 2B). In control samples vacuolar H^+-ATPase localized in the cytoplasm and was evident as spots in most cells. Treatment with the inhibitor caused a more homogeneous and diffuse distribution of the enzyme.

Migration, invasion and wound healing. The effect of NiK-12192 on H460 cell migration and invasion was investigated after 24 h of drug exposure to concentrations not affecting cell adhesion (Fig. 3). All cells (control or NiK-12192-treated) were trypan blue negative. Under these conditions, NiK-12192 caused a concentration-dependent inhibition of cell migration and invasion.

To further support the ability of NiK-12192 to modulate cell migration, we examined the drug effect in wound healing, because this assay provides information on oriented migration involving cell polarization. As shown in Fig. 4, during 48 h incubation control cells were able to repair about 50% the wound. NiK-12192, at a low subtoxic concentration (0.5 μM), caused a

JPET Fast Forward. Published on October 1, 2007 as DOI: 10.1124/jpet.107.128587
This article has not been copyedited and formatted. The final version may differ from this version.

reduction in the wound healing.

Modulation of factors related to cell-cell interactions. Since the αvβ3 integrin is highly expressed in lung carcinoma cells (Albert et al., 2006) and associations between integrins and vacuolar H^+-ATPase have been already reported (Lee et al., 2004), the intracellular localization of αvβ3 was investigated in H460 cells following treatment. As shown in Fig. 5, in untreated cells the integrin was found mainly polarized in the cell cytoplasm, whereas in treated cells αvβ3 was more homogeneously diffused in the cytoplasm, thus suggesting a different behavior of treated cells in cell-cell and cell-matrix interactions.

The effect of the vacuolar H^+-ATPase inhibitor on proteins of cytoskeleton was examined by confocal microscopy (Fig. 6). In this analysis, actin was evidenced as green filaments and tubulin as red filaments. In control cells, long and regular fibers of tubulin in the cell cytoplasm and filaments of actin forming pseudopodia were found. Marked modifications were found in H460 cells exposed to NiK-12192 (2 μM) for 24 h. In treated cells, actin fibers were broken and spots of aggregation were evident. Moreover, no pseudopodia and lack of regular structure for actin filaments could be observed.

The drug ability to interfere with three-dimensional growth of H460 cells was examined on agar substratum, because this effect may have relevance in the metastatic growth. Spheroids with a diameter of 100-150 μm were treated with subtoxic concentrations of the drug and their size was then determined at various exposure times (Fig. 7). In spheroids treated with NiK-12192, a concentration-dependent inhibition growth was found already at 24 h also with the low concentration (0.5 μM).

Antitumor and antimetastatic activity of NiK-12192. To determine whether the

JPET Fast Forward. Published on October 1, 2007 as DOI: 10.1124/jpet.107.128587
This article has not been copyedited and formatted. The final version may differ from this version.

inhibitory activity on invasion/migration observed in *in vitro* systems by NiK-12192 was reflected in a drug effect on *in vivo* invasiveness of tumor cells, we examined the occurrence of spontaneous lung metastases in mice s.c. implanted with H460 cells following drug treatment (Table 1). Mice were treated with NiK-12192, 30 mg/kg, daily (5 times/week), by oral gavage for 62 days. At day 63, mice were sacrificed for lung observation and, even though all mice presented lung metastasis, the mean number of macroscopic metastases was significantly reduced in treated mice versus controls, with 42% inhibition ($P<0.01$). A comparable effect on the extent of metastases was found after treatment with topotecan (1 mg/kg, daily, per os), a well known cytotoxic drug. The therapeutic efficacy of the two drugs was increased by their combination, being the number of lung metastases inhibited to 81% versus control mice ($P<0.01$), and such inhibition was also significantly different *vs* those achieved by single agent-treated mice ($P<0.05$, at least). Both NiK-12192 and topotecan only partially inhibited growth of the primary s.c. tumors, even though at a significant level ($P<0.01$ vs control tumors). Their combined treatment achieved an effect which was much more significant compared to control tumors ($P<0.0005$), but not significant vs single agent-treated tumors (Fig 8). No lethal toxicity nor body weight loss higher than 5% were observed in all treated groups.

To further get insight into the steps of the metastatic process affected by NiK-12192, we examined the drug effects on experimental lung metastases, i.e. induced by i.v. injection of H460 ascitic cells, thus bypassing the first steps of the metastatic process. Mice were treated per os with NiK-12192, 30 mg/kg, according to the same schedule and for spontaneous metastasis experiment (for 7 weeks) and sacrificed for lung observation at day 83 (Table 1). At such a time, all mice in the control group presented a large metastatic burden and most of them had tumor-invaded lungs; no relevant differences could be observed in the NiK-12192-treated mice. In contrast, topotecan was able to significantly reduce the number of lung metastases ($P<0.05$ vs

control mice). Interestingly, the combination of NiK-12192 and topotecan resulted in an even higher inhibition of the metastases number vs control mice ($P<0.01$) and in the lack of metastasis in 1 out of 7 mice.

Since angiogenesis, in particular the migration of microvascular endothelial cells, is known to be regulated by extracellular pH (Orive et al., 2003, Rojas et al., 2006), the effect of NiK-12912 treatment on tumor neovascularization was investigated in primary s.c. growing H460 tumors treated daily (30 mg/kg) for 2 weeks (Fig. 9). Tumor angiogenesis appeared only marginally reduced by treatment with NiK-12192, being the MVD of treated tumors lower compared to that of control tumors (30% inhibition, but not significantly different). Topotecan, according to the daily schedule of treatment, showed a higher antiangiogenic activity (42% inhibition, $P<0.01$) and the combined treatment achieved a somewhat higher MVD inhibition (52%, $P<0.005$ vs control).

Discussion

The results presented in the study indicated that the vacuolar H^+-ATPase inhibitor NiK-12192 was able to reduce the migration/invasion of H460 cells in vitro and significantly reduce the number of spontaneous metastases in the lung of nude mice s.c. implanted with a human lung carcinoma. The ability of our model to produce spontaneous metastases which is a unique feature among s.c.-implanted human tumor xenografts, is of particular relevance, because it may represent a behaviour more closely related to the clinical dissemination of tumor cells. It has been shown that some steps of the complex process leading to the formation of spontaneous metastases are dependent on extra and intracellular pH, including the secretion of acid-dependent proteases and the local degradation of basement membranes and extracellular matrix (Rozhin et al., 1994;

Martinez-Zaguilan et al., 1996; Stock et al., 2005; Rofstad et al., 2006). Indeed, the acidic pH of extracellular microenvironment of solid tumors has been shown to be a critical factor in stimulating tumor cells motility, invasion and angiogenesis (Harguindey et al., 2005).

In spite of the significant inhibition of the metastatic potential of s.c. growing H460 tumor, NiK-12192 exhibited a marginal effect on the development of artificial metastases (i.e. following i.v. injection of the same tumor cells). The poor effect shown by NiK-12192 against artificial lung metastases and primary tumor supports the hypothesis that the compound was able to inhibit the early steps of the metastatic process, rather than the tumor cell growth in the target organ.

We have previously shown, either in cellular and in *in vivo* systems, that NiK-12192 is able to potentiate topotecan efficacy against human colon carcinomas, possibly by a cytoplasmic redistribution of the cytotoxic drug, and by modulating the expression of membrane-associated transport systems (Petrangolini et al., 2006). In the present study we showed that the combination topotecan+NiK-12192 resulted in a significant reduction of spontaneous metastasis incidence over that achieved by each single drug. The mechanisms of antimetastatic effects of NiK-12192 and topotecan are substantially different. The effects of topotecan were likely related to its cytotoxic activity, because both spontaneous and artificial metastases were inhibited by the topotecan treatment. However, the antimetastatic effect of topotecan could reflect multiple events including a direct tumor growth inhibition and an early antiangiogenic effect, which could account for the topotecan efficacy in reducing both spontaneous and artificial metastases. The antiangiogenic effects of topotecan in primary tumor could at least in part account for the synergistic inhibition of spontaneous metastasis by the topotecan+NiK-12192 combination. The angiogenic effects of camptothecins have been already described and are more evident when the drugs are delivered by the daily low-dose schedule (Petrangolini et al., 2003). The effect of NiK-

12192 on microvessel density, which may be expected on the basis of the knowledge that a significant number of angiogenic factors acts closely related to intracellular H^+ dynamics (Orive et al., 2003), was marginal as compared to that achieved by the cytotoxic drug, suggesting that the antiangiogenic effect is not a primary mechanism of antimetastatic activity.

In the previous study an increased toxicity was achieved by the combination topotecan+NiK-12192, when topotecan maximum tolerated dose (every 4^{th} day for 3 times) was delivered (Petrangolini et al., 2006). Thus, a different regimen was investigated in the present study, i.e., a daily low-dose for long time. Such regimen was well tolerated and, in spite of the prolonged time of treatment (up to 9 weeks), no signs of toxicity (nor lethal toxicity, nor body weight loss) were observed in mice treated with topotecan+NiK-12192, thus indicating that the toxicity of the combination can be modulated in this regimen.

The ability of NiK-12192 to inhibit vacuolar H^+-ATPase activity appears to influence a number of cellular functions, which may be relevant to the observed antimetastatic efficacy in the *in vivo* studies. Indeed, the results achieved in the *in vitro* assays support the ability of NiK-12192 to modulate the intracellular pH and to inhibit a series of metastasis-associated events. Our results indicated that in H460 cells NiK-12192 was able to cause cytoskeleton modifications, including aggregation of actin and tubulin microfilament as well as reduction of cell pseudopodia. In addition, it was able to modulate the subcellular distribution of adhesion molecules such as $\alpha v\beta 3$ integrin. The reduced cell motility was reflected in the inhibition of cell migration, invasion and likely in wound healing. Several lines of evidence have indicated a relation among cellular functions involving transport systems, cytoskeleton and adhesion molecules (Vitavska et al., 2003; Zuo et al., 2006). These functions, which may be modulated by intracellular and extracellular pH, play a critical role in cellular interactions with the extracellular

matrix. A lot of evidences suggested important interactions among vacuolar H^+-ATPase and cytoskeleton: the aminoterminal domain of the vacuolar H^+-ATPase subunit B has been already demonstrated to contain a filamentous actin binding site (Holliday et al., 2000; Zuo et al., 2006), and the vacuolar H^+-ATPase subunit C can bind both F and G-actin (Vitavska et al., 2005), by controlling the dynamics of the actin cytoskeleton. A modification of the cytoskeleton has been in fact observed in our model following a 24 h treatment with NiK-12192, resulting in a lack of regular structure for actin filaments together with the absence of pseudopodia.

Vacuolar H^+-ATPases are implicated in multiple diseases, including osteoporosis, deafness and cancer, and their role as drug target is under study (Bowman and Bowman, 2005). A recent study reported the efficacy of another vacuolar H^+-ATPase inhibitor, FR202126, in reducing osteolysis induced by a metastatic breast cancer in a syngenic mouse model. However, the compound was unable to prevent lung or liver metastasis (Niikura, 2006). It is unclear if the drug specificity for various vacuolar H^+-ATPase isoforms expressed in different cells (including osteoclasts) may be responsible for the different effects of these inhibitors. The ability of the natural macrolide vacuolar H^+-ATPase inhibitor bafilomycin A1 to decrease *in vitro* both invasion and migration of human breast metastatic cells (Sennoune et al., 2004b), strongly supports the key role of vacuolar H^+-ATPase in these two fundamental processes of tumor malignancy. The implication of the enzyme in modulation of the metastatic phenotype is supported by the observation that cells with a low metastatic potential are characterized by a widespread distribution of the enzyme in cytoplasm. Relevant to this point is the NiK-12192-induced modulation of intracellular distribution of the enzyme.

In conclusion, we have shown for the first time that a vacuolar H^+-ATPase inhibitor, NiK-12192, has a strong antimetastatic effect in a preclinical model of spontaneous lung metastases. Moreover, the effect was further increased by the combination with a cytotoxic drug, thus

supporting a potential interest for vacuolar H^+-ATPase inhibitors in the therapy of cancer.

References

Albert JM, Cao C, Geng L, Leavitt L, Hallahan DE and Lu B (2006) Integrin $\alpha_v\beta_3$ antagonist cilengitide enhances efficacy of radiotherapy in endothelial cell and non-small-cell lung cancer models. *Int J Rad Oncol Biol Phys* **65**:1536-1543.

Belotti D, Vergani V, Drudis T, Borsotti P, Pitelli MR, Viale G, Giavazzi R and Taraboletti G (1996) The microtubule-affecting drug paclitaxel has antiangiogenic activity. *Clin Cancer Res* **2**:1843-1849.

Bowman EJ and Bowman BJ (2005) V-ATPases as drug targets. *J Bioenerg Biomembr* **37**:431-435.

Cassinelli G, Lanzi C, Petrangolini G, Tortoreto M, Pratesi G, Cuccuru G, Laccabue D, Supino R, Belluco S, Favini E, Poletti A and Zunino F (2006) Inhibition of c-Met and prevention of spontaneous metastatic spreading by the 2-indolinone RPI-1. *Mol Cancer Ther* **5**:1-10.

Corti C, Pratesi G, De Cesare M, Pelligrini R, Giardini R, Supino R and Zunino F (1996) Spontaneous lung metastases in a human lung tumor xenograft: a new experimental model. *J Cancer Res Clin Oncol* **122**:154-160.

Farina C, Gagliardi S, Nadler G, Morvan M, Parini C, Belfiore P, Visentin L and Gowen M (2001) Novel bone antiresponsive agents that selectively inhibit the osteoclast V-H^+-ATPase. *Farmaco* **56**:113-116.

Harguindey S, Orive G, Pedraz JL, Paradiso A and Reshkin SJ (2005) The role of pH dynamics and the Na^+/H^+ antiporter in the etiopathogenesis and treatment of cancer. Two faces of the same coin – one single nature. *Biochim Biophys Acta* **1756**:1-24.

Holliday LS, Lu M, Lee BS, Nelson RD, Solivan S, Zhang L and Gluck SL (2000) The amino-terminal domain of the B subunit of vacuolar H+-ATPase contains a filamentous actin

binding site. *J Biol Chem* **275**:32331-32337.

Lee I, Skinner MA, Guo H, Sujan A and Pierce M (2004) Expression of the vacuolar H^+-ATPase 16-kDa subunit results in the triton X-100-insoluble aggregation of β_1 integrin and reduction of its cell surface expression. *J Biol Chem* **279**:53007-53014.

Liang C-C, Park AY and Guan J-L (2007) *In vitro* scratch assay: a convenient and inexpensive method for analysis of cell migration *in vitro*. *Nature Protocols* **2**:329-333.

Liotta LA and Stetler-Stevenson WG (1993) Principles of molecular cell biology of cancer: cancer metastasis, in *Cancer Principles & Practice of Oncology* (DeVita VT, Hellman S and Rosenberg SA eds.), pp. 134-149, JB Lippincott Co., Philadelphia.

Lu X, Qin W, Li J, Tan N, Pan D, Zhang H, Xie L, Yao G, Shu H, Yao M, Wan D, Gu J and Yang S (2005) The growth and metastasis of human hepatocellular carcinoma xenografts are inhibited by small interfering RNA targeting to the subunit ATP6L of proton pump. *Cancer Res* **65**:6843-6849.

Marcotte N, Brouwer AM (2005) Carboxy SNARF-4F as a fluorescent pH probe for ensemble and fluorescence correlation spectroscopies. *J Phys Chem* 109:11819-11828.

Martinez-Zaguilan R, Lynch RM, Martinez GM and Gillies RJ (1993) Vacuolar-type H^+-ATPases are functionally expressed in plasma membranes of human tumor cells. *Am J Physiol Cell Physiol* **265**:1015-1029.

Martinez-Zaguilan R, Martinez GM, Gomez A, Hendrix MJ and Gillies RJ (1998) Distinct regulation of pH^{in} and $[Ca^{2+}]^{in}$ in human melanoma cells with different metastatic potential. *J Cell Physiol* **176**:196-205.

Martinez-Zaguilan R, Seftor EA, Seftor REB, Chu Y, Gillies RJ and Hendrix MJC (1996) Acidic pH enhances the invasive behaviour of human melanoma cells. *Clin Exp Metastasis*

14:176-186.

Niikura K (2006) Effect of a v-ATPase inhibitor, FR202126, in syngeneic mouse model of experimental bone metastasis. Cancer Chemother Pharmacol, published online.

Ohta T, Numata M, Yagishita H, Futagami F, Tsukioka Y, Kitagawa H, Kayahara M, Nagakawa T, Miyazaki I, Yamamoto M, Iseki S and Ohkuma S (1996) Expression of 16 kDa proteolipid of vacuolar-type H(+)-ATPase in human pancreatic cancer. *Br J Cancer* **73**:1511-1517.

Orive G, Reshkin SJ, Harguindey S and Pedraz JL (2003) Hydrogen ion dynamics and the Na^+/H^+ exchanger in cancer angiogenesis and antiangiogenesis. *Br J Cancer* **89**:1395-1399.

Petrangolini G, Pratesi G, De Cesare M, Supino R, Pisano C, Marcellini M, Giordano V, Laccabue D, Lanzi C and Zunino F (2003) Antiangiogenic effects of the novel camptothecin ST1481 (Gimatecan) in human tumor xenografts. *Mol Cancer Res* **1**:863-870.

Petrangolini G, Supino R, Pratesi G, Dal Bo L, Tortoreto M, Crove AC, Misiano P, Belfiore P, Farina C and Zunino F (2006) Effect of a novel vacuolar-H^+-ATPase inhibitor on cell and tumor response to camptothecin. *J Pharm Exp Ther* **318**:939-946.

Putnam RW (2001) Intracellular pH regulation. In *Cell Physiology Source-Book: A molecular approach, 3rd edition* (Sperelakis N ed) pp. 357-376, Academic Press, San Diego.

Rofstad EK, Mathiesen B, Kindem K and Galappathi K (2006) Acidic extracellular pH promotes experimental metastasis of human melanoma cells in athymic nude mice. *Cancer Res* **66**:6699-6707.

RojasJD, Sennounw SR, Maiti D, Bakunts K, Reuveni M, Sanka SC, Martinez GM, Seftor EA, Meininger CJ, Wu G, Wesson DE, Hendrix MJ and Martinez-Zaguilan R (2006) Vacuolar-type H+-ATPases at the plasma membrane regulate pH and cell migration in microvascular endothelial cells. *Am J Physiol Heart Circ Physiol* **291**:1147-1157.

Rozhin J, Sameni M, ZieglerG and Slone BF (1994) Pericellular pH affects distribution and secretion of cathepsin B in malignant cells. *Cancer Res* **54**:6517-6525.

Sennoune SR, Luo D and Martinez-Zaguilan R (2004a) Plasma-lemmal vacuolar-type H^+-ATPase in cancer biology. *Cell Biochem Biophys* **40**:185-206.

Sennoune SR, Bakunts K, Martinez GM, Chua-Tuan JL, Kebir Y, Attaya MN and Martinez-Zaguilan R (2004b) Vacuolar H+-ATPase in human breast cancer cells with distinct metastatic potential: distribution and functional activity. *Am J Physiol Cell Physiol* **286**:1443-1452.

Stock C, Gassner B, Hauck CR, Arnold H, Mally S, Eble JA, Dieterich P and Schwab A (2005) Migration of human melanoma cells depends on extracellular pH and Na^+/H^+ exhange. *J Physiol* **567.1**:225-238.

Vitavska O, Merzendorfer H and Wieczorek H (2005) The V-ATPase subunit C binds to polymeric F-Actin as well as to monomeric G-actin and induces cross-linking of actin filaments. J Biol Chem 280:1070-1076.

Vitavska O, Wieczorek H and Merzendorfer H (2003) A novel role for subunit C in mediating binding of the H+-V-ATPase to the actin cytoskeleton. *J Biol Chem* **278**:18499-18505.

Workman P, Twentyman P, Balkwill F, Balmain A, Chaplin D, Double J, Embleton J, Newell D, Raymond R, Stables J, Stephens T and Wallace J (1998) United kingdom Co-ordinating Committee on Cancer Research (UKCCR) guidelines for the welfare of animals in experimental Neoplasia (2 edn). *Br J Cancer* **77**:1-10.

Zuco V, Zanchi C, Cassinellu G, Lanzi C, Supino R, Pisano C, Zanier R, Giordano V, Garattini E and Zunino F (2004) Induction of apoptosis and stress response in ovarian carcinoma cell lines treated with ST1926, an atypical retinoid. *Cell Death Differ* **11**:280-289.

Zuo J, Jiang J, Chen SH, Vergara S, Gong Y, Xue J, Huang H, Kaku M and Holliday LS (2006)

Actin binding activity of subunit B of vacuolar H+-ATPase is involved in its targeting to ruffled membranes of osteoclasts. *J Bone Miner Res* **21**:714-721.

Footnotes

This work was partially supported by the Associazione Italiana Ricerca sul Cancro, Milan, and by the Ministero della Salute, Rome, Italy.

Legends for Figures

Fig. 1. Intracellular pH modulation by NiK-12192 in H460 cells. SNARF-4F fluorescence spectra were recorded in single cells from NiK-12192 treated and untreated samples at 366 nm excitation and 550-800 nm interval emission. Each spectrum derives from a single cell. Three spectra are reported for treated samples. Only one spectrum is reported for control cells, due to the homogeneous results.

Fig. 2. Vacuolar H^+-ATPase expression and subcellular localization in H460 cells. A: Western blot analysis performed on nitrocellulose filters incubated with anti-vacuolar H^+-ATPase D primary antibody and peroxidase conjugated anti-rabbit antibodies. Actin was used as control of loading. 1, untreated control; 2, cells treated with NiK-12192 (2 μM) for 24 h. B: Subcellular localization as by fluorescence microscopy in H460 cells untreated or treated with NiK-12192 (2 μM) for 24 h and stained with anti-vacuolar H^+-ATPase D antibody and with the FITC-secondary anti-rabbit antibody.

Fig. 3. Adhesion, migration and invasion in NiK-12192 treated H460 cells. After 24 h of exposure to NiK-12192 cells were seeded in trans-well plates with membranes coated with (invasion) or without (migration) matrigel, as reported in Materials and Methods. Data indicate the percentages (+/- S.D.) of adherent, migrated, or invaded cells in comparison with untreated samples; data are derived from two independent experiments performed in duplicate.

Fig. 4. Effect of NiK-12192 on wound healing of H460 cell monolayers after scratching.

Monolayers of H460 cells were scratched and treated with NiK-12192 (0.5 μM). At 48 h the distance between the rims of the scratching was measured by an Image Analysis System. Pictures of the same samples at different times after scratching are reported and are representative of three different regions from a single wound.

Fig. 5. αvβ3 intracellular localization in H460 cells. After 24 h of exposure to NiK-12192 (2 μM), cells were incubated with αvβ3 monoclonal antibody and stained with secondary FITC-antibody. Pictures were taken by fluorescence microscope at 500x.

Fig. 6. Effect of NiK-12192 on cytoskeleton proteins. Images of H460 cells double-stained with anti-tubulin monoclonal antibody followed by Alexa-594 conjugated anti mouse (red) and FITC-phalloidin (actin fibers, green) obtained by sequential scanning with confocal laser microscope. The third panel of each raw represents the merge of green and red channels; one out of 24-34 frames is shown. Long and regular fibers of tubulin in the cell cytoplasm and filaments of actin forming pseudopodia are visible in control cells (upper row). In H460 cells after 24 h of drug exposure (2 μM), actin and tubulin fibers looked unstructured and spots of aggregation were evident (lower row). Scale bar = 10 μm.

Fig. 7. Effect of NiK-12192 on the three-dimensional growth of H460 spheroids. Single spheroids were grown in 96-well plates. Measures of spheroid diameters were taken by a micrometer lens in an inverted microscope at various times. Values are reported as percentage of the diameter length over that of time 0. Each point is referred to mean value (+/- S.D.) of six spheroids. Control (■); NiK-12192, 0.5 μM (▼); NiK-12192, 2 μM (●).

JPET Fast Forward. Published on October 1, 2007 as DOI: 10.1124/jpet.107.128587
This article has not been copyedited and formatted. The final version may differ from this version.

Fig. 8. Effect of NiK-12192 on the growth of primary H460 tumor. Mice were implanted s.c. with H460 lung cancer cells ($2x10^6$ cells/mouse) and treated per os with solvent (x); 1 mg/kg topotecan (TPT) (○); 30 mg/kg NiK-12192 (□); TPT + NiK-12192 (▲). Treatments were delivered daily from day 1, 5 days/week, for 9 weeks. TPT was delivered about 1 h before NiK-12192. Means of 9-11 tumors/group are reported.

Fig. 9. Microvessel density (MVD) in H460 tumor xenografts. Mice implanted s.c. with H460 lung cancer cells ($2x10^6$ cells/mouse) were treated per os with solvent (control) or topotecan (TPT, 1 mg/kg), or NiK-12192 (30 mg/kg) or TPT+NiK-12192. Treatments were delivered daily, from day 1 for 2 weeks. Topotecan was delivered about 1 h before NiK-12192. The day after the last treatment, tumors were excised and fixed in 10% buffered formalin for hematoxylin-eosin staining. MVD was assessed in 3 fields, at 400x, within non necrotic areas. Means of 3-4 tumors/group (± SD) are reported. *P<0.01; **P<0.005 vs control.

TABLE 1

Effects of NiK-12192 (30 mg/kg/injection) and topotecan (1 mg/kg/injection), alone or in combination, on spontaneous and artificial lung metastases of H460 human lung tumor xenograft

Drug[a]	Weeks of[b] treatment	Animals with metastases/ total no. of animals	No. of spontaneous metastases[c]				No. of artificial metastases[c]		
			Mean	Median	Range	Inhib. %[d]	Mean	Median	Range[e]
Solvent	9	11/11	26	17	5-80	-			
	7	6/ 6					338	400	21-500
NiK-12192	9	10/10	15***	11	3-56	42			
	7	7/ 7					300	300	104-500
Topotecan	9	9/ 9	11***	11	4-23	58			
	7	7/ 7					65*	10	3-300
Topotecan+NiK-12192	9	10/10	5***,f	5	1- 9	81			
	7	6/ 7					49**	4	0-300

[a]Topotecan and NiK-12192 were delivered per os by gavage. When combined, topotecan was delivered about 1 h before NiK-12192.

[b]Drug were administered daily x5/week.

[c]Counted in the lungs when mice were sacrificed, i.e. day 63 for spontaneous metastases and day 83 for artificial metastases.

[d]Inhibition % compared to solvent-treated mice.

[e]One lung-lobe totally invaded was calculated as 100 metastases. Totally invaded lungs are reported as 500.

*<0.05, **<0.02, ***<0.01 vs control; [f]<0.05 vs single-agent-treated mice, by Mann-Whitney rank test.

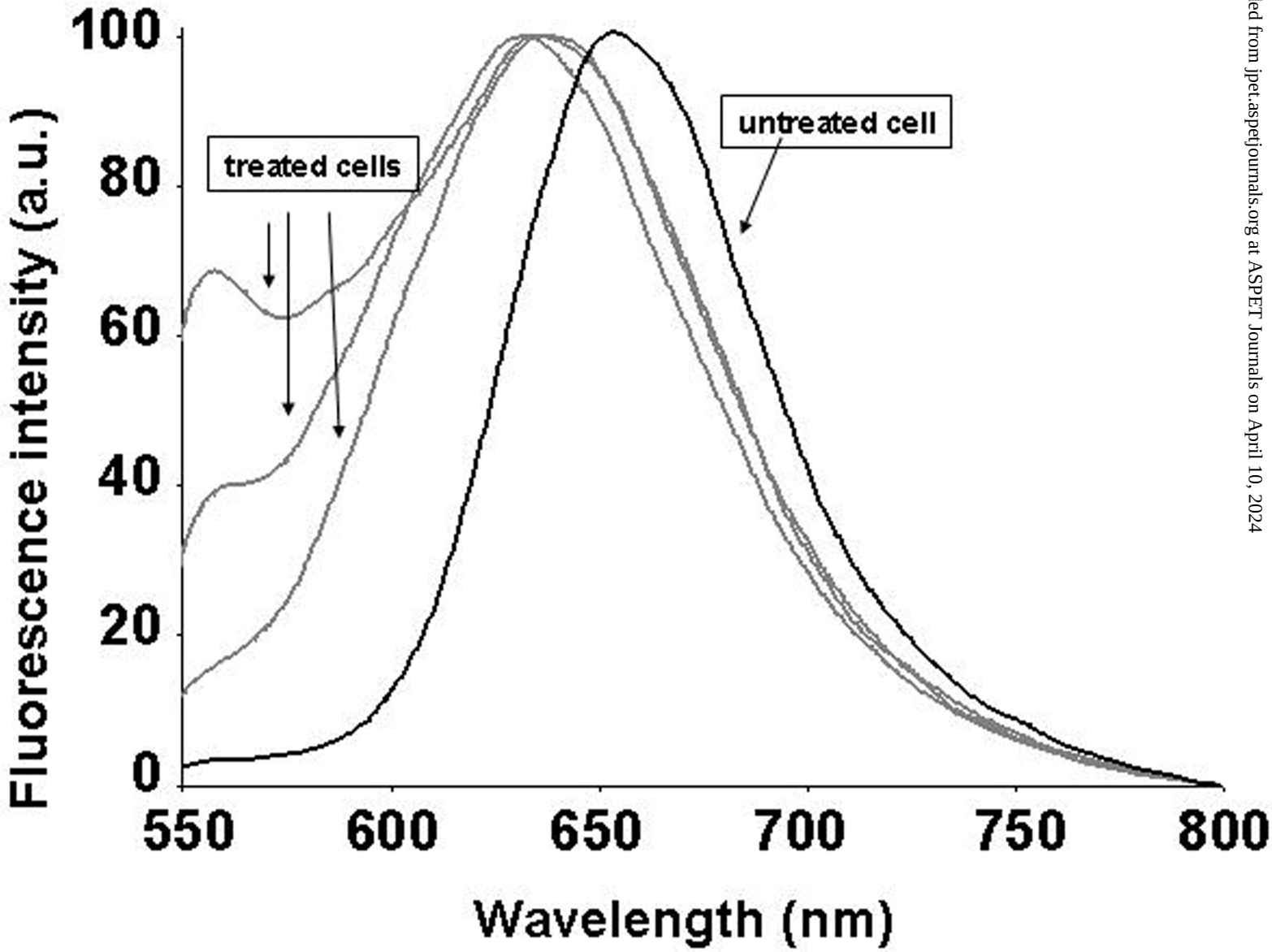

Figure 1

A

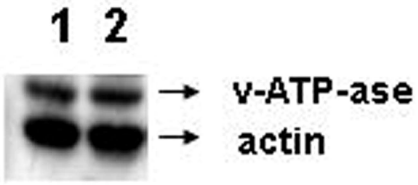

B

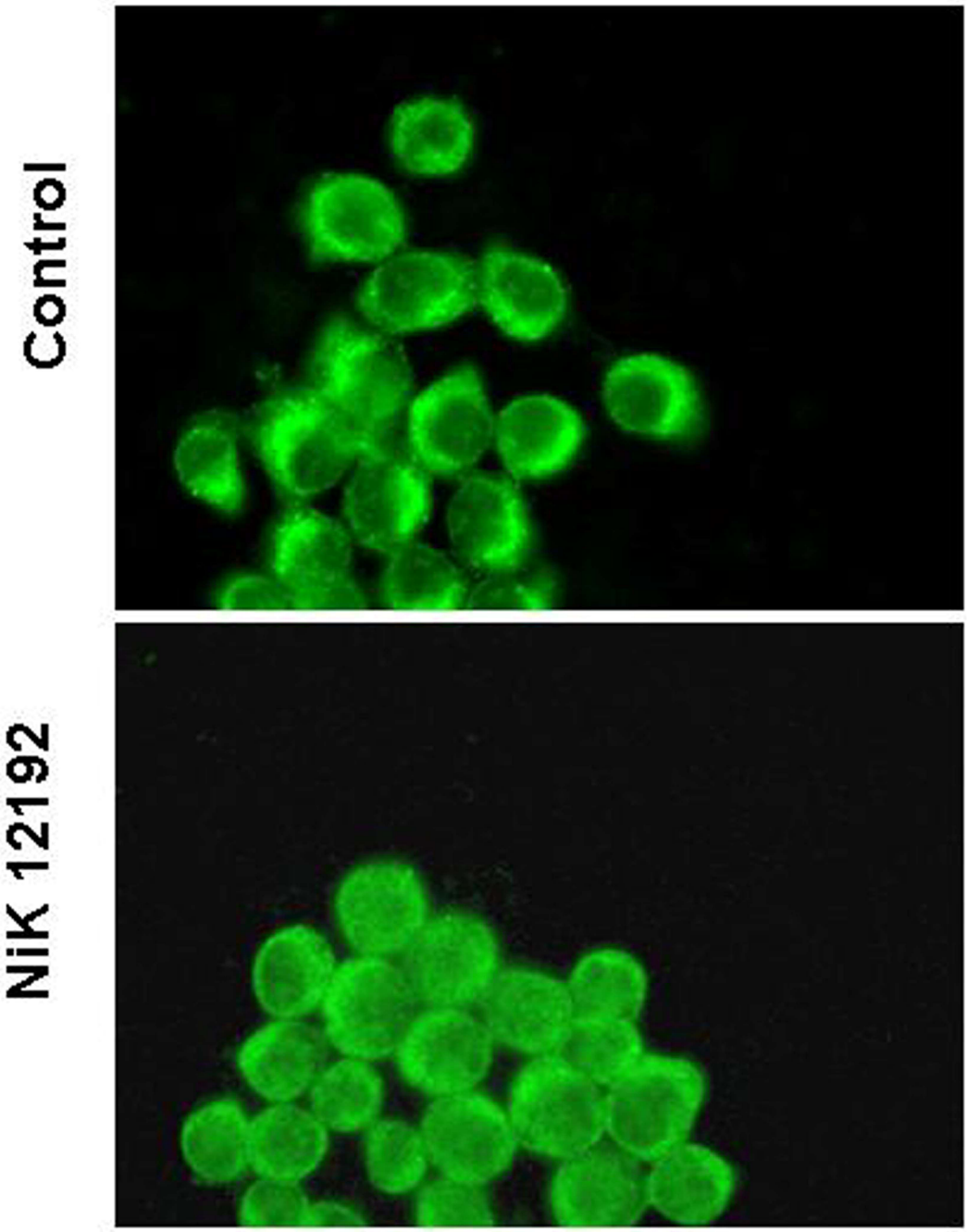

Figure 2

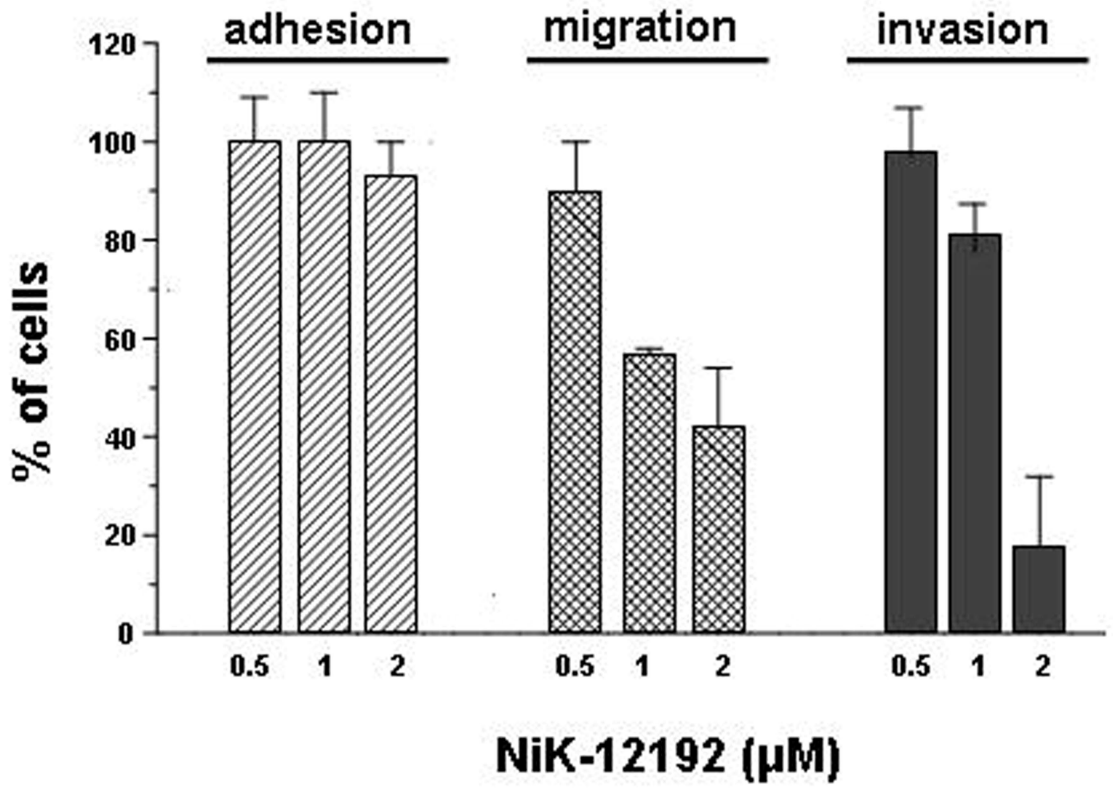

Figure 3

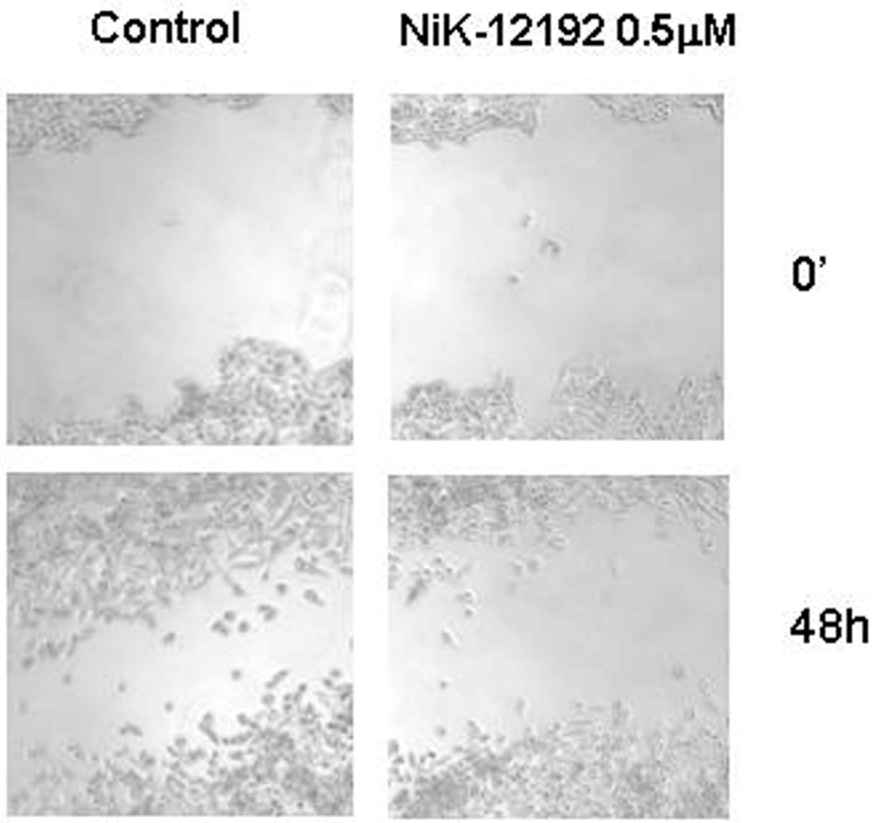

Figure 4

NiK-12192

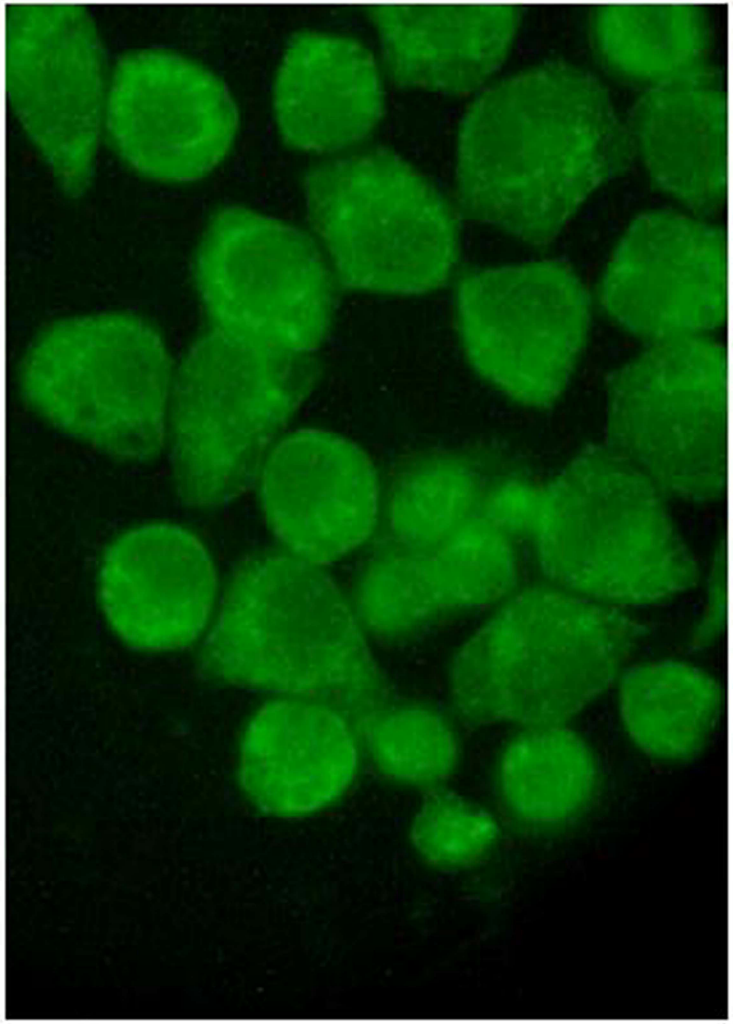

Control

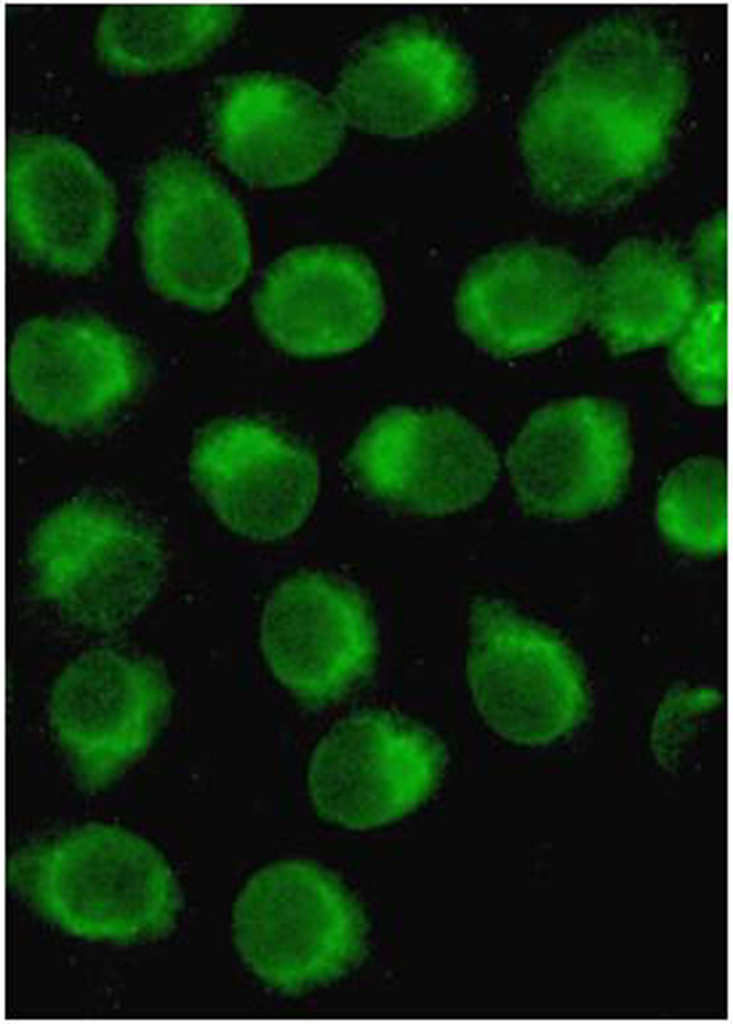

Figure 5

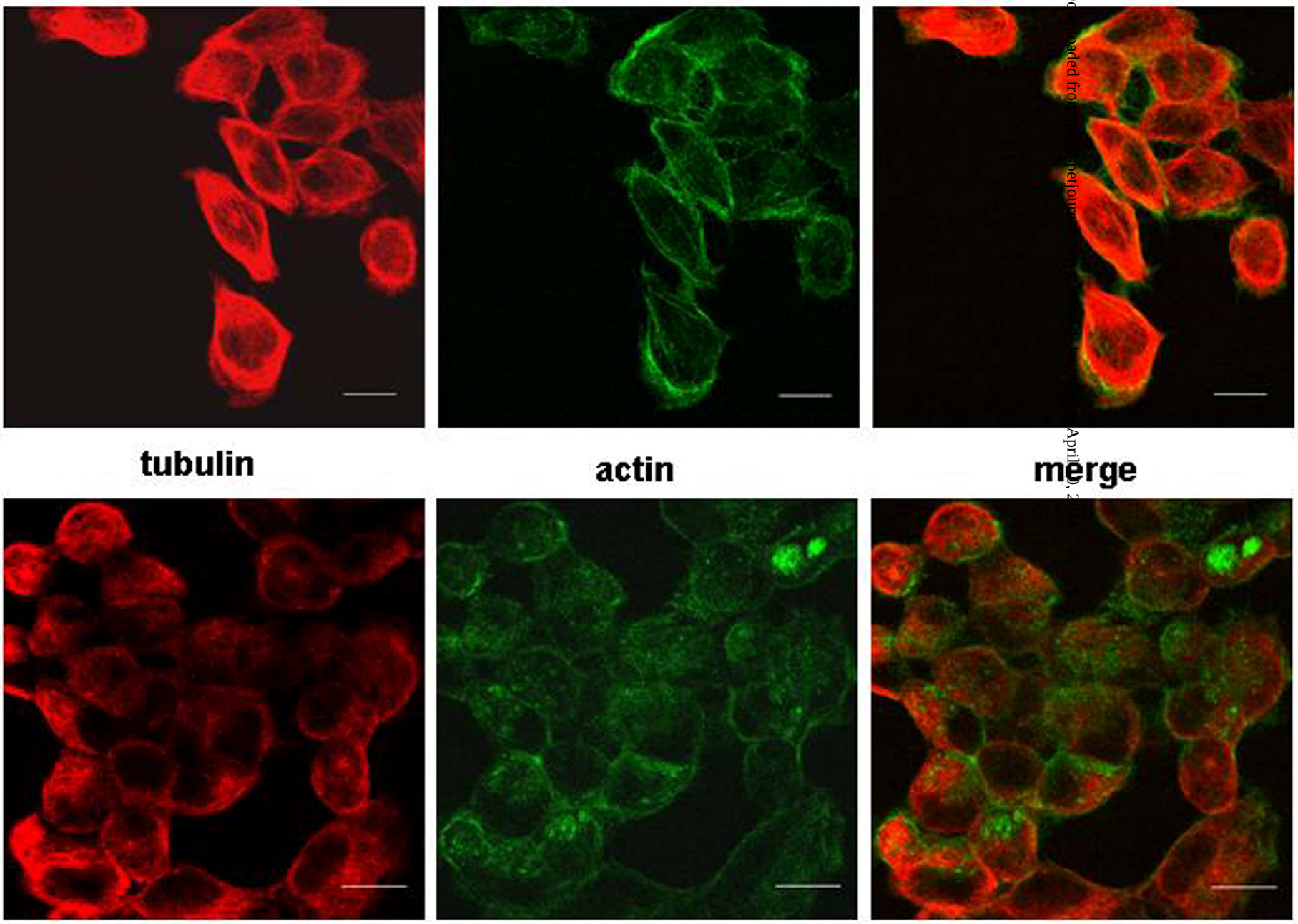

Figure 6

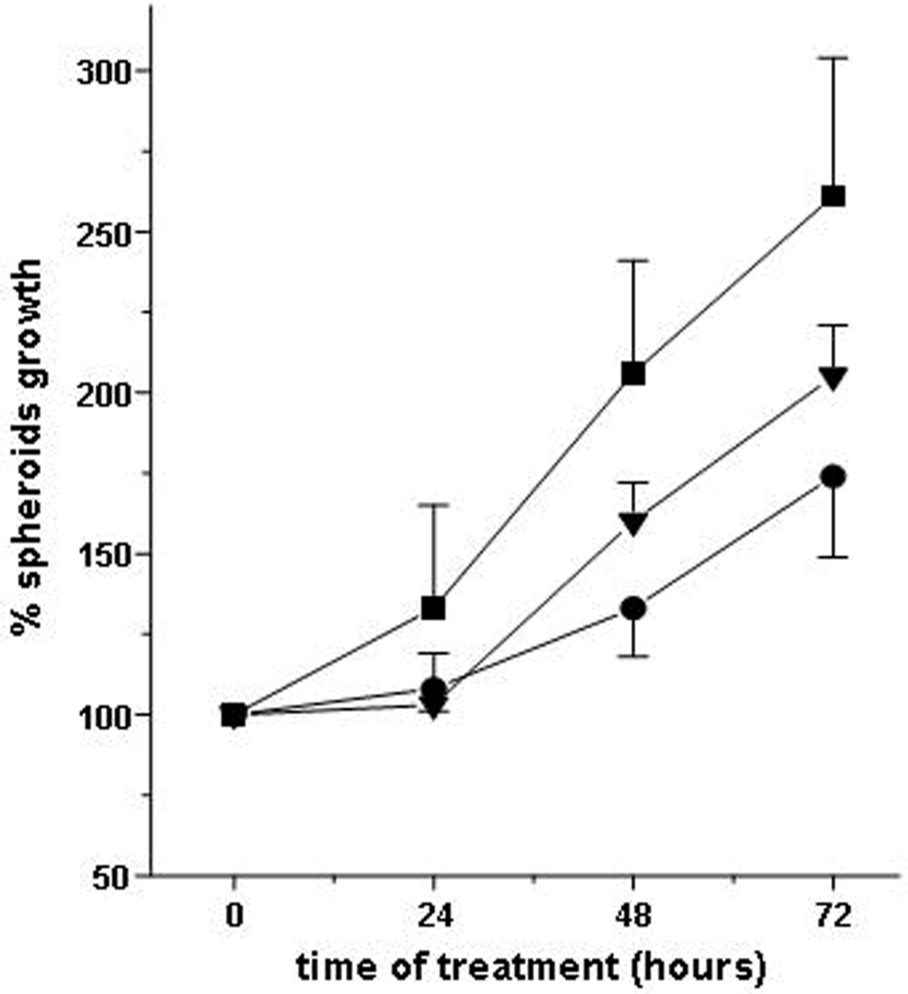

Fig. 7

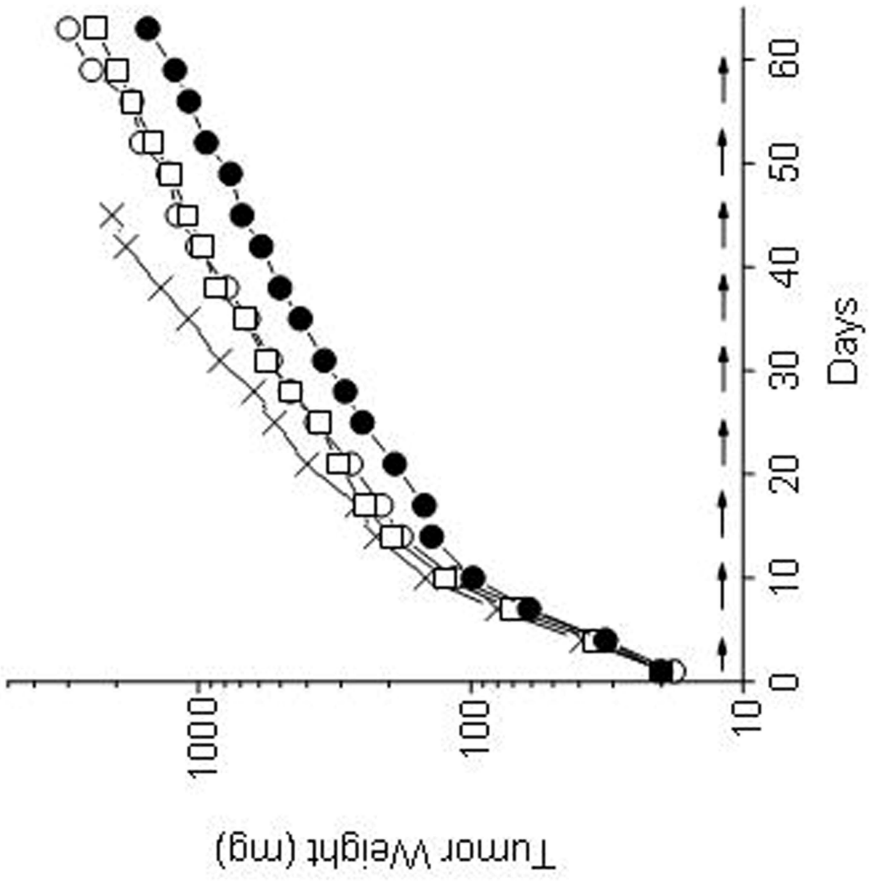

Figure 8

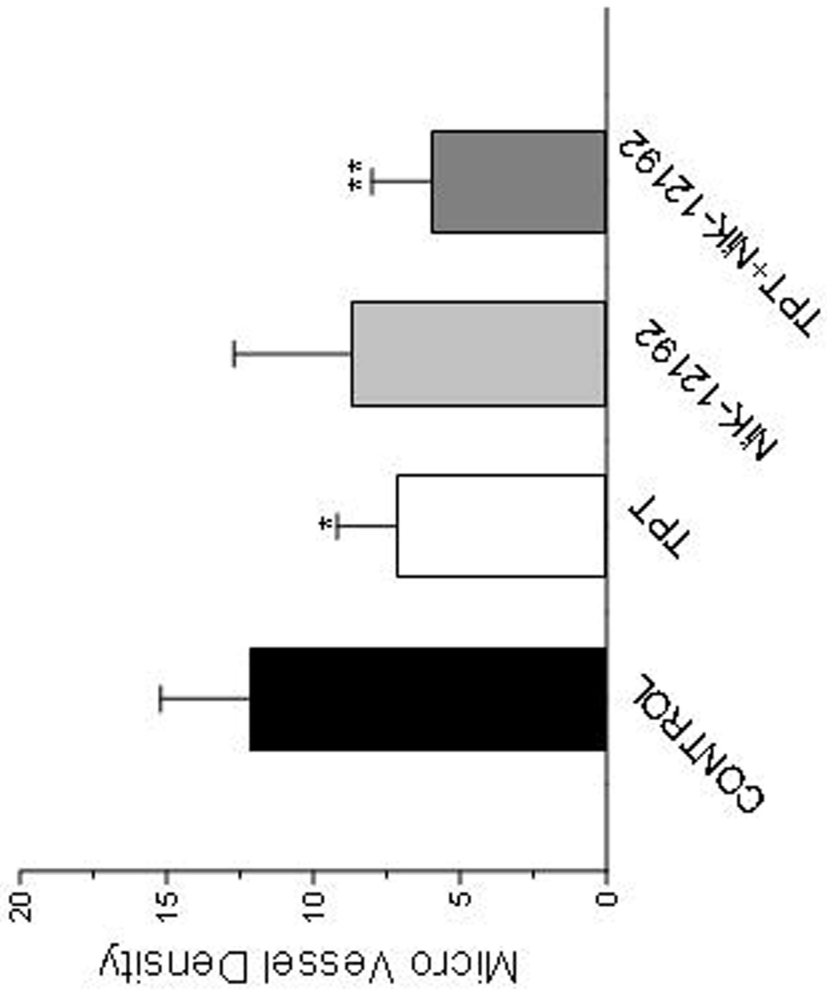

Figure 9